

Effects of the buffer layer on the Casimir pressure of peptide films deposited on a substrate

Dingding Lv(吕丁丁), Shuai Zhou(周帅), Kaipeng Liu(柳开鹏), Shiwei Dai(戴士为), and Lixin Ge(葛力新)
Citation: Chin. Phys. B, 2025, 34 (**10**): 104202. DOI: 10.1088/1674-1056/adde36
http://cpb.iphy.ac.cn; http://iopscience.iop.org/cpb

What follows is a list of articles you may be interested in

Electromagnetically-induced-absorption-like ground state cooling in a hybrid optomechanical system

Yaoyong Dong(董耀勇), Xuejun Zheng(郑学军), Denglong Wang(王登龙), and Peng Zhao(赵鹏)
Chin. Phys. B, 2025, 34 (**4**): 044203. DOI: 10.1088/1674-1056/adb260

Quantum-state engineering using enhanced tripartite interactions in atom-photon-phonon hybrid systems

Yaowu Guo(郭耀武), Jiaqiang Zhao(赵加强), Lianzhen Cao(曹连振), Yingde Li(李英德), and Hong-Yan Lu(路红艳)
Chin. Phys. B, 2025, 34 (**2**): 024203. DOI: 10.1088/1674-1056/ad9a5d

Giant enhancement of negative friction by resonant coupling between localized surface phonon polaritons and graphene plasmonics

Kaipeng Liu(柳开鹏), Shuai Zhou(周帅), Shiwei Dai(戴士为), and Lixin Ge(葛力新)
Chin. Phys. B, 2025, 34 (**1**): 014202. DOI: 10.1088/1674-1056/ad886c

Enhanced mechanical squeezing in an optomechanical system via backward stimulated Brillouin scattering

Shan-Shan Chen(陈珊珊), Yi-Long Xie(谢亦龙), Jing-Jing Zhang(张京京), Na-Na Zhang(张娜娜), Yong-Rui Guo(郭永瑞), Huan Yang(杨桓), and Yong Ma(马勇)
Chin. Phys. B, 2025, 34 (**1**): 014201. DOI: 10.1088/1674-1056/ad8cc0

Presentation of the Berry-Tabor conjecture in Lévy plates

Chao Li(李超) and Guo-Lin Hou(侯国林)
Chin. Phys. B, 2024, 33 (**10**): 104204. DOI: 10.1088/1674-1056/ad21f2

Effects of the buffer layer on the Casimir pressure of peptide films deposited on a substrate

Dingding Lv(吕丁丁)[1], Shuai Zhou(周帅)[1,3], Kaipeng Liu(柳开鹏)[1], Shiwei Dai(戴士为)[2], and Lixin Ge(葛力新)[1,†]

[1] *School of Physics and Electronic Engineering, Xinyang Normal University, Xinyang* 464000, *China*
[2] *College of Mathematics and Physics, Chengdu University of Technology, Chengdu* 610059, *China*
[3] *Department of Basic Courses, Zhengzhou University of Science and Technology, Zhengzhou* 450064, *China*

(Received 30 March 2025; revised manuscript received 14 May 2025; accepted manuscript online 29 May 2025)

The Casimir pressure plays an important role in the adhesion stability of nanofilms at submicro scales. In this work, the Casimir pressure of peptide films deposited on a layered substrate is investigated. Three types of semi-infinite substrates, i.e., silica, silicon and gold, are considered. The buffer layer between the peptide film and substrate consists of silicon or silica. The switching sign of the Casimir pressure can be controlled in a region ranging from about 130 nm to 1000 nm, depending on the thickness of the buffer layer and the substrate. The results suggest that the critical thickness of peptide films for Casimir equilibrium increases (or decreases) by increasing the thickness of the silicon (or silica) buffer film. The influences of wetting and electrolyte screening on the Casimir pressure are also investigated. Our finding provides a theoretical guide for the adhesion stability of peptide films in organic electronics.

Keywords: Casimir pressure, buffer layer, peptide films, electrolyte screening

PACS: 42.50.Lc, 87.14.ef, 61.20.Qg

DOI: 10.1088/1674-1056/adde36 **CSTR:** 32038.14.CPB.adde36

1. Introduction

During the past two decades, organic electronics have made great progress, for example in organic thin-film transistors,[1,2] organic solar cells,[3–5] organic light-emitting diodes,[6–8] etc. It is well known that organic materials consist of carbon-based small organic molecules or polymers. Organic films are the basic building blocks of organic electronics, and are of great importance in many kinds of devices. The organic film is generally deposited on an inorganic substrate, and the stability of the organic film is strongly influenced by the surface forces (such as ionic or electrostatic forces, hydrogen bonding, hydrophilic forces, etc.) at the interfaces. The dispersion force,[9] among several other surface forces,[10] plays an important role when the thickness of the organic film reduces to the submicro scale.

The dispersion force is attributed to the zero-point vacuum fluctuation and thermal fluctuation. For two closely spaced objects, or two interfaces, the dispersion force is known as the van der Waals force,[11] and the relativistic retardation is negligible. When the separation is large, the retardation effect becomes evident and the dispersion force is called the Casimir force or the Casimir–Lifshitz force.[12,13] The Casimir force and its free energy have been investigated in various fields[14,15] such as nanomechanics,[15–19] optical cavities,[20–23] quantum manipulations (dynamical Casimir effects),[24–26] premelting of ice,[27–29] etc. In addition, the adhesive stability of organic films due to the Casimir force has also been reported (e.g., for DNA films[30] and peptide films[31]). When peptide films are deposited on different substrates (e.g., metal,[32–34] silica[34,35] or semiconductor[36]), repulsive or attractive Casimir forces are revealed depending on the type of substrate and the thickness of the peptide film. However, previous studies have mainly focused on semi-infinite substrates. The Casimir force of peptide films deposited on multi-layer substrates is still unexplored.

In this work, we study the Casimir pressure of peptide films deposited on a layered substrate. Three kinds of semi-infinite substrates, i.e., silica, silicon and gold, are considered. The buffer layer between the peptide film and substrate consists of silicon or silica. For a non-metallic substrate, the Casimir pressure is repulsive when the peptide film is thin while it can be attractive when the thickness of the peptide film is large. Moreover, the switching sign of the Casimir pressure can be controlled via the thickness of the buffer layer deposited on a proper substrate. We find that the critical thickness of peptide films for Casimir equilibrium increases when the thickness of the silicon buffer film is increased. By contrast, the critical thickness of peptide films shows an inverse trend with the silica buffer film. For a silica-coated gold substrate, the Casimir pressure could be attractive within a specific range of peptide film thickness, and can be strongly tuned by the buffer layer thickness. We also show that modulation of Casimir pressure due to wetting and electrolyte screening can

†Corresponding author. E-mail: lixinge@hotmail.com

© 2025 Chinese Physical Society and IOP Publishing Ltd. All rights, including for text and data mining, AI training, and similar technologies, are reserved.

be manifested under specific conditions.

2. Theoretical models

We consider a peptide film with thickness a deposited on a layered substrate. The layered substrate consists of a buffer film (medium 1) with permittivity ε_1 placed on a semi-infinite slab (medium 2) with permittivity ε_2. The Casimir pressure of the peptide film is calculated based on the framework of the Lifshitz theory[13,31]

$$P_{\rm c}(d) = -\frac{k_{\rm B}T}{\pi}\sum_{n=0}^{\infty'} k_{||}k_{\rm pz}\,{\rm d}k_{||}\left(\frac{r_{\rm t}^{\rm TE}r_{\rm b}^{\rm TE}{\rm e}^{-2k_{\rm pz}a}}{1-r_{\rm t}^{\rm TE}r_{\rm b}^{\rm TE}{\rm e}^{-2k_{\rm pz}a}} + \frac{r_{\rm t}^{\rm TM}r_{\rm b}^{\rm TM}{\rm e}^{-2k_{\rm pz}a}}{1-r_{\rm t}^{\rm TM}r_{\rm b}^{\rm TM}{\rm e}^{-2k_{\rm pz}a}}\right). \quad (1)$$

Note that the prime in the summation denotes a prefactor $1/2$ for the term $n=0$, $k_{\rm B}$ is the Boltzmann constant, T is the temperature, $k_{\rm pz}=\sqrt{k_{||}^2+\varepsilon_{\rm p}({\rm i}\xi_n)\,\xi_n^2/c^2}$ is the vertical wavevector in the peptide film, $k_{||}$ is the parallel wavevector, c is the speed of light in a vacuum, $\varepsilon_{\rm p}({\rm i}\xi_n)$ is the permittivity of the peptide film, $\xi_n=2\pi\frac{k_{\rm B}T}{\hbar}n$ ($n=0,\,1,\,2,\,3$) are the discrete Matsubara frequencies, $\hbar$ is the reduced Planck constant and r_β^α ($\alpha=$ TE, TM; $\beta={\rm t,b}$) are the reflection coefficients for the peptide film, where the superscripts TE and TM correspond to the polarizations of transverse electric and transverse magnetic modes, respectively. The subscripts t and b denote the reflection coefficients of the peptide at the top and bottom interfaces, respectively.

For the top interface, the reflection coefficients represent an electromagnetic wave incident from the peptide film to the air (or vacuum)[31]

$$r_{\rm t}^{\rm TM}({\rm i}\xi_n,k_{||}) = \frac{k_{\rm pz}({\rm i}\xi_n,k_{||})-\varepsilon_{\rm p}({\rm i}\xi_n)k_{0z}({\rm i}\xi_n,k_{||})}{k_{\rm pz}({\rm i}\xi_n,k_{||})+\varepsilon_{\rm p}({\rm i}\xi_n)k_{0z}({\rm i}\xi_n,k_{||})}, \quad (2)$$

$$r_{\rm t}^{\rm TE}({\rm i}\xi_n,k_{||}) = \frac{k_{\rm pz}({\rm i}\xi_n,k_{||})-k_{0z}({\rm i}\xi_n,k_{||})}{k_{\rm pz}({\rm i}\xi_n,k_{||})+k_{0z}({\rm i}\xi_n,k_{||})}, \quad (3)$$

where $k_{0z}=\sqrt{k_{||}^2+\xi_n^2/c^2}$ is the vertical wavevector in air.

For the bottom interface of the peptide film, the reflection coefficients can be given as[37,38]

$$r_{\rm b}^{\alpha} = \frac{r_{\rm p1}^{\alpha}+r_{12}^{\alpha}{\rm e}^{-2k_{1z}L}}{1+r_{\rm p1}^{\alpha}r_{12}^{\alpha}{\rm e}^{-2k_{1z}L}}, \quad (4)$$

where L is the thickness of the buffer film, $r_{\rm p1}^{\alpha}$ is the reflection coefficient from the peptide film to the buffer layer and r_{12}^{α} is the reflection coefficient from the buffer layer to the semi-infinite slab, and we have

$$r_{\rm p1}^{\rm TM}({\rm i}\xi_n,k_{||}) = \frac{\varepsilon_1({\rm i}\xi_n)k_{\rm pz}({\rm i}\xi_n,k_{||})-\varepsilon_{\rm p}({\rm i}\xi_n)k_{1z}({\rm i}\xi_n,k_{||})}{\varepsilon_1({\rm i}\xi_n)k_{\rm pz}({\rm i}\xi_n,k_{||})+\varepsilon_{\rm p}({\rm i}\xi_n)k_{1z}({\rm i}\xi_n,k_{||})}, \quad (5)$$

$$r_{\rm p1}^{\rm TE}({\rm i}\xi_n,k_{||}) = \frac{k_{\rm pz}({\rm i}\xi_n,k_{||})-k_{1z}({\rm i}\xi_n,k_{||})}{k_{\rm pz}({\rm i}\xi_n,k_{||})+k_{1z}({\rm i}\xi_n,k_{||})}, \quad (6)$$

$$r_{12}^{\rm TM}({\rm i}\xi_n,k_{||}) = \frac{\varepsilon_2({\rm i}\xi_n)k_{1z}({\rm i}\xi_n,k_{||})-\varepsilon_1({\rm i}\xi_n)k_{2z}({\rm i}\xi_n,k_{||})}{\varepsilon_2({\rm i}\xi_n)k_{1z}({\rm i}\xi_n,k_{||})+\varepsilon_1({\rm i}\xi_n)k_{2z}({\rm i}\xi_n,k_{||})}, \quad (7)$$

$$r_{12}^{\rm TE}({\rm i}\xi_n,k_{||}) = \frac{k_{1z}({\rm i}\xi_n,k_{||})-k_{2z}({\rm i}\xi_n,k_{||})}{k_{1z}({\rm i}\xi_n,k_{||})+k_{2z}({\rm i}\xi_n,k_{||})}, \quad (8)$$

where $k_{jz}=\sqrt{k_{||}^2+\varepsilon_j({\rm i}\xi_n)\,\xi_n^2/c^2}$ ($j=1,2$) is the vertical wavevector in media 1 and 2, respectively. For example, when the peptide film is deposited on a silica substrate with a silicon film as the buffer layer, media 1 and 2 represent the materials silicon and silica, respectively. The reflection coefficients for layered structures can be calculated alternatively by a transfer matrix method.[39,40] Clearly, the reflections for the TE modes would be zero when the Matsubara term $n=0$.

The dielectric functions of the materials are significant for the reflection coefficients. Here, the permittivity of the dry peptide is taken from Ref. [31]. The permittivities of silicon, silica, water and gold are taken from a recent publication,[41] which accounts for the influences of the electronic dielectric constant, optical bandgap, density and chemical composition of the materials. For a wet peptide film, the permittivity $\varepsilon_{\rm p}'$ is given as[31]

$$\frac{\varepsilon_{\rm p}'({\rm i}\xi_n)-1}{\varepsilon_{\rm p}'({\rm i}\xi_n)+2} = \Phi\frac{\varepsilon_{\rm w}'({\rm i}\xi_n)-1}{\varepsilon_{\rm w}'({\rm i}\xi_n)+2} + (1-\Phi)\frac{\varepsilon_{\rm p}'({\rm i}\xi_n)-1}{\varepsilon_{\rm p}'({\rm i}\xi_n)+2}, \quad (9)$$

where $\varepsilon_{\rm w}({\rm i}\xi_n)$ represents the permittivity of water[35] and Φ is the volume fraction of water in the peptide film.

3. Results and discussion

The dielectric functions of the materials used evaluated in the imaginary frequency are shown in Fig. 1(a). For the Matsubara term $n>0$, the permittivity of the peptide is smallest compared with substrate materials of silica and silicon. The permittivity of water is larger than that of the peptides while it is smaller than that of the substrate materials. To predict the behavior of Casimir pressures, the $n=0$ Matsubara term is significant since it plays a dominant role at large thicknesses (or separation), as reported in Refs. [31,42]. The static permittivities of the water and peptide are about 81 and 15, respectively. For a wet peptide, the static permittivity lies between 15 and 22.9 when the fraction of water increases from 0 to 0.4. On the other hand, the static permittivities of silica and silicon are about 3.9 and 11.7, respectively, which are smaller than that of the peptide film.

When a peptide film is deposited on a semi-infinite silica or intrinsic semiconducting substrate,[31,36] the Casimir pressure would be repulsive at a small thickness (or separation) since the relationship $\varepsilon_{\rm air}<\varepsilon_{\rm p}<\varepsilon_{\rm sub}$ is satisfied for a vast range of frequencies.[43] However, the Casimir pressure turns out to be attractive at a large peptide thickness because of the breakdown of the above relationship for the dominant term $n=0$. As a result, a stable Casimir equilibrium, i.e., when the pressure equals zero, can be found due to the counterbalance of the

repulsive and attractive Casimir forces. It is expected that the Casimir equilibria could be tuned accordingly when the layer thicknesses of substrates are artificially designed.[44]

Figure 1(b) shows the Casimir pressure of a peptide film deposited on a silica substrate with a silicon film as the buffer layer. The calculations show that the Casimir force is repulsive and it declines with increasing thickness a. The Casimir equilibrium appears at a critical thickness of the peptide film, depending on the thickness of the buffer film. The critical thickness of peptide film for Casimir equilibrium is denoted as a_0. As the thickness of the silicon film L decreases from 500 nm to 20 nm, the critical thickness a_0 declines from about 900 nm to 300 nm. It has been reported that a_0 generally appears at several micrometers for semi-infinite semiconductor substrates.[36] Here, we find that the critical thickness a_0 can be greatly reduced by decreasing the thickness of the buffer film. Hence, a thin silicon film is favored for the adhesion stability of peptide films at submicro scales.

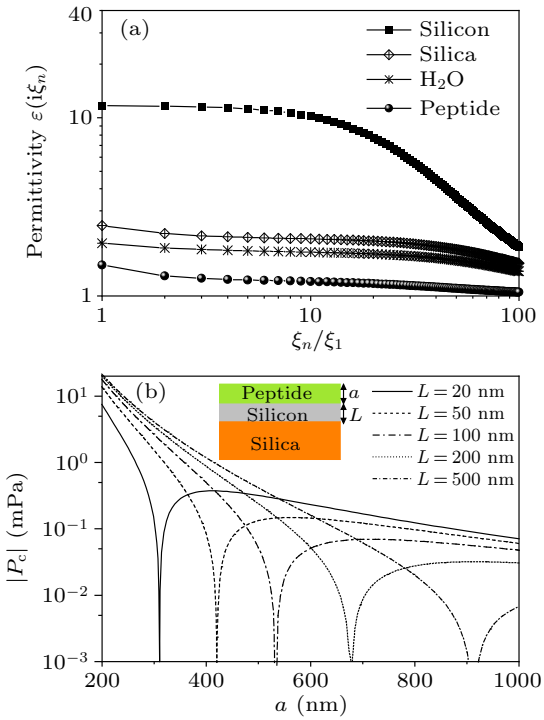


Fig. 1. (a) The permittivity of the materials used as a function of normalized Matsubara frequency. (b) The magnitude of Casimir pressures as a function of the thickness of the peptide film under different silicon nanofilm thicknesses.

Now we turn to the other type of layered substrate, wherein a silica film is the buffer layer between the peptide film and semi-infinite silicon. The Casimir pressure versus the thickness of the peptide film is shown in Figs. 2(a) and 2(b). When the layer of silica is thick, for example 600 nm, the Casimir pressure is almost the same as that of semi-infinite silica. As the thickness of the buffer layer decreases to 400 nm and 200 nm, the Casimir pressure tends to be more repulsive, and the critical thickness a_0 increases correspondingly. As the thickness of silica declines further from 120 nm to 60 nm, the thickness a_0 increases from 300 nm to 900 nm, as shown in Fig. 2(b). It is expected that the lower stability due to the decreasing thickness of the silica layer can be compensated by adding a graphene sheet on the peptide film or coating with nanoparticles.[32,33] Nonetheless, the variation of the silica buffer film thickness provides an avenue for tuning the stability of peptide films.

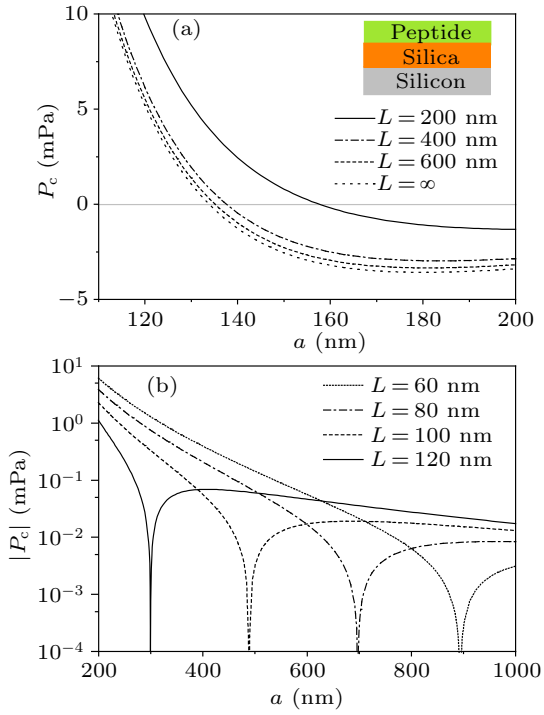


Fig. 2. The Casimir pressure for a peptide film placed on a silica-coated silicon slab. (a) The silica film thickness increases from 200 nm to infinite. (b) The silica film thickness increases from 60 nm to 120 nm.

It would be interesting to investigate the Casimir interactions of wet peptide films deposited on a layered substrate. The Casimir pressures under different fractions of water are shown in Fig. 3(a) for a silicon film as the buffer layer. We set the thickness $L_{\mathrm{Si}} = 20$ nm, and the corresponding critical thickness a_0 is near 300 nm. The results show that the Casimir pressure is modified correspondingly when the fraction of water changes. The Casimir pressure for $\Phi = 0.2$ is larger (smaller) than the dry case for a smaller (larger) peptide film thickness, and a_0 for these two configurations are very close. On the other hand, the Casimir pressure for $\Phi = 0.4$ shows a more significant discrepancy compared with the dry film.

Next, we consider a layered substrate consisting of a silica buffer film deposited on a semi-infinite silicon substrate. Figure 3(b) show the Casimir pressures under different fractions of water, where the thickness $L_{\mathrm{SiO_2}} = 120$ nm and the Casimir equilibrium is also near 300 nm. The Casimir pressure tends to be more attractive as the volume fraction increases. Clearly, the modulation of the Casimir pressures due to the wetting effect in this configuration is much larger than that in Fig. 3(a).

When the volume fraction Φ increases from 0 to 0.2, the critical thickness a_0 declines from about 300 nm to 250 nm. For $\Phi = 0.4$, the thickness a_0 decreases further to about 182 nm. The modulation of critical thickness due to the change of Φ from 0 to 0.4 lies in the region of about 180–300 nm, which is much larger than in the case of semi-infinite silica.[34]

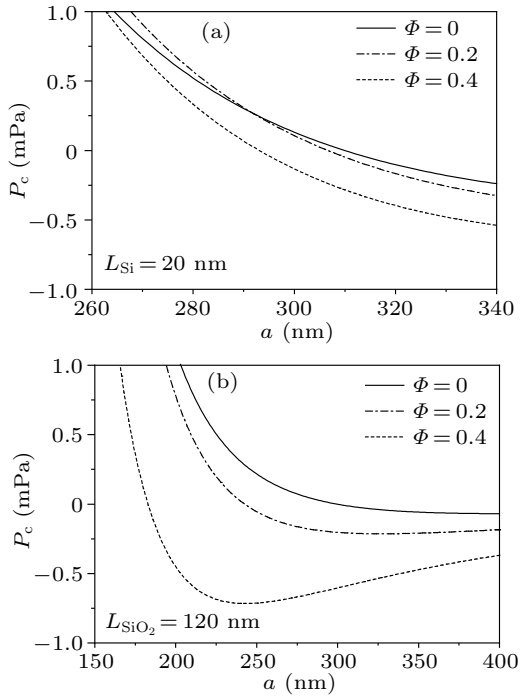


Fig. 3. The Casimir pressure under different water volume fractions. The layered substrates are (a) a silicon film placed on semi-infinite silica and (b) a silica film placed on semi-infinite silicon.

Water is considered as a dielectric medium for the above discussions. However, water is an electrolyte solution in realistic systems, and the effect of electrolyte screening should be taken into account.[23] Due to ionic charge fluctuations, the presence of salt ions in water (e.g., H^+, OH^-, Na^+, etc.) can modify the $n = 0$ Matsubara term. As a result, the vertical wavevector for a wet peptide film turns out to be $k_{pz} = \sqrt{k_{||}^2 + \kappa^2}$ in Eq. (1) for the reflection coefficient of the TM mode with the Matsubara term $n = 0$, where the wavevector $\kappa = 1/\lambda_D$ with λ_D being the Debye length.[11] The Debye length is dependent on the concentration of the ions, the temperature, the static permittivity of the wet peptide film, etc. For example, the Debye length is about 1000 nm for pure water at room temperature,[45] resulting from the H^+ and OH^- ions. Adding a small amount of NaCl to water reduces the Debye length from approximately 1000 nm to 10 nm as the NaCl concentration increases from 10^{-7} mol·L^{-1} to 10^{-3} mol·L^{-1}.[23] When salted water mixes with a peptide film the configuration becomes more complex. The Debye length depends not only on the concentration of salt in the water but also on the water volume fraction in peptide film. Qualitatively, the Debye length would decline with increasing salt concentration (e.g., NaCl) in the water.

The Casimir pressure for a wet peptide film is shown in Figs. 4(a) and 4(b) under different Debye lengths. The solid lines represent cases of nonionic configurations. Our results indicate that electrolyte screening has a small influence on the Casimir pressure when the condition $a \ll \lambda_D$ is satisfied. In other words, the electrolyte screen can be neglected for a thin peptide film with low-salt water. However, as the thickness of the peptide film becomes comparable to or even larger than λ_D, strong modulation of the Casimir pressure is revealed due to the screening effect. We find that the Casimir equilibrium is shifted when the Debye length is reduced from 1000 nm to 500 nm. As λ_D decreases to 100 nm, the Casimir equilibrium is absent and the Casimir interaction turns out to be monotonic in Fig. 4(a). The situation is similar for a substrate of silica buffer film placed on semi-infinite silicon, as shown in Fig. 4(b). The results suggest that the stability of the peptide film decreases with a reduction in the Debye length (e.g., via increased salt concentration).

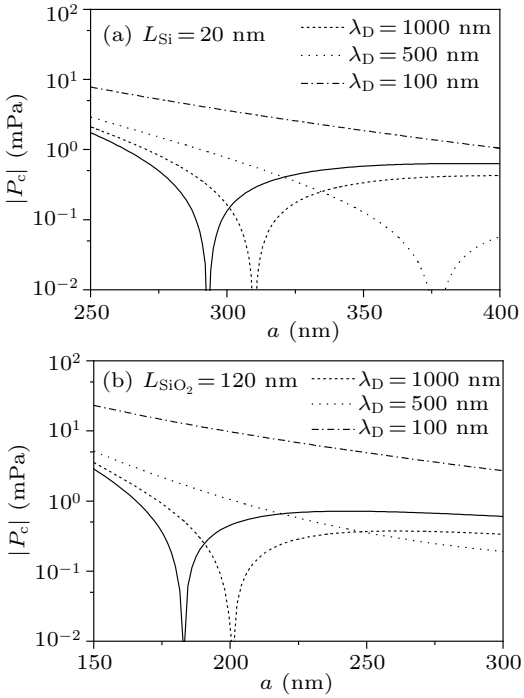


Fig. 4. The Casimir pressure across wet peptide films under different Debye lengths. The layered substrates are (a) a silicon film placed on semi-infinite silica and (b) a silica film placed on semi-infinite silicon. The water volume fraction is fixed at 0.4. The solid lines represent the case without accounting for the electrolyte screening effect.

Finally, we consider the Casimir pressure of a peptide film placed on a gold substrate. The permittivity of gold is high for broadband frequencies. Unlike the case of silica or silicon, the permittivity of gold is larger than that of the peptide for both $n = 0$ and $n > 0$ terms. Hence, the Casimir pressure of the peptide film is long-range repulsive when it is placed on a gold substrate, as reported in Ref. [31]. It would be useful if the Casimir pressure could become attractive when a buffer layer is introduced between a peptide film and a gold substrate. Contour plots of Casimir pressure with regard to the thicknesses of

the buffer layer and peptide film are shown in Figs. 5(a) and 5(b), where the buffer layer is silica. The pressure is normalized by $P_0 = \hbar c\pi^2/(240d^4)$, which is the Casimir pressure between two perfect metal slabs. These results suggest that the Casimir pressure across a dry peptide film is long-range repulsive when the thickness of the buffer layer is less than about 200 nm. This is because the repulsive Casimir interaction between the peptide film and gold substrate is dominant for a thin buffer layer. As the thickness of silica increases further, for example to 300 nm, the Casimir pressure versus the thickness a has two equilibria. This means that the Casimir pressure is attractive within a specific range of peptide film thicknesses. For a wet peptide, the Casimir pressure tends to be more attractive than for a dry one. A negative Casimir pressure could even be found with a thinner buffer layer, as shown in Fig. 5(b).

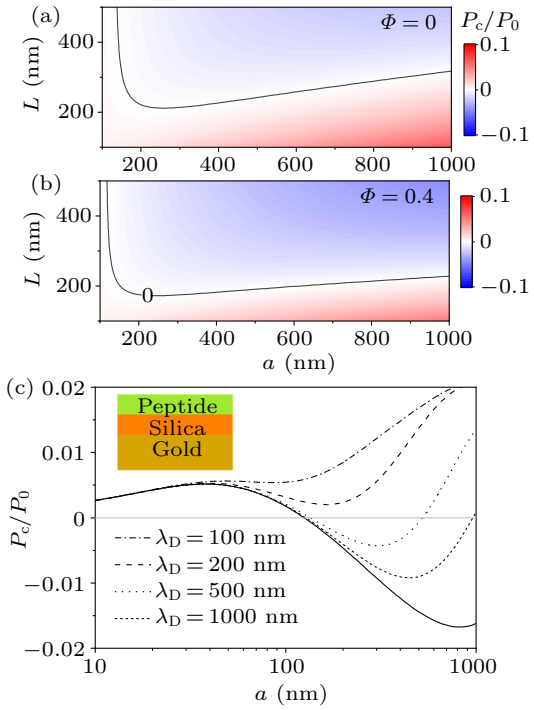


Fig. 5. Contour plot of Casimir pressure for a peptide film placed on a silica-coated gold substrate: (a) dry peptide film and (b) wet peptide film. (c) The Casimir pressure for the wet peptide film ($\Phi = 0.4$) under different Debye lengths, wherein the solid line represents the case without accounting for the electrolyte screening effect. The thickness of the buffer layer in (c) is fixed at 300 nm.

Figure 5(c) shows the Casimir pressure for a wet peptide film when screening from ionic charge fluctuation is taken into account. The solid lines represent cases that do not account for ionic charge fluctuation. For a thin peptide film, the Casimir pressure is unaffected by the screening effect. However, the Casimir pressure trends to be repulsive for a large thickness a, and peptide films become less stable with decreasing Debye length λ_D. The Casimir pressure is attractive within a specific range of a when λ_D is 500 nm and 1000 nm. The critical thickness a_0 for the first Casimir equilibrium is almost unchanged when λ_D is large, such as 500 nm or 1000 nm. When λ_D decreases to 200 nm and 100 nm, the Casimir equilibria disappear and the Casimir pressure is long-range repulsive.

4. Conclusion and perspectives

In summary, this work focuses on the Casimir pressures of a peptide film deposited on layered substrates. The influence of the buffer layer on the Casimir pressure is investigated for different substrates. For a non-metallic substrate, the Casimir pressure is repulsive when the peptide film is thin, while the pressure can be attractive when the film is thick. The critical thickness of peptide films for Casimir equilibrium increases with enlarging the thickness of the silicon buffer film. By contrast, the critical thickness decreases with increasing the thickness of the silica buffer film. The critical thickness of peptide film for switching signs of the Casimir pressure can be artificially controlled in a region ranging from about 130 nm to 1000 nm, depending on the thicknesses of the buffer layer and substrates. The influences of the fraction of water contained in the peptide films and the electrolyte screen are discussed. A strong modulation of the Casimir pressure is revealed when the Debye length is comparable to the thickness of the peptide film. For a metallic substrate, the different trends of Casimir pressure across the peptide films are also revealed and discussed. Alternative buffer materials to silicon and silica[46,47] (such as Teflon, ZnMgO and hexagonal BN), may offer different controls over Casimir interactions due to their distinct dielectric properties. Moreover, the temperature effect in the system could have a non-negligible influence on the Casimir pressure, which would an interesting direction for future works. Our finding provides a theoretical guide to the adhesion stability of peptide films placed on organic electronics.

Acknowledgements

Project supported by the National Natural Science Foundation of China (Grant No. 11804288) and the Natural Science Foundation of Henan (Grant No. 232300420120).

References

[1] Chen H, Zhang W, Li M, He G and Guo X 2020 *Chem. Rev.* **120** 2879
[2] Dimitrakopoulos C D and Malenfant P R L 2002 *Adv. Mater.* **14** 99
[3] Riede M, Spoltore D and Leo K 2021 *Adv. Energy Mater.* **11** 2002653
[4] Duan L and Uddin A 2020 *Adv. Sci.* **7** 1903259
[5] Zhang K, Song P, Ma F and Li Y 2024 *Chin. Phys. B* **33** 068402
[6] Jeon S O, Lee K H, Kim J S, Ihn S G, Chung Y S, Kim J W, Lee H, Kim S, Choi H and Lee J Y 2021 *Nat. Photonics* **15** 208
[7] Reineke S, Thomschke M, Lüssem B and Leo K 2013 *Rev. Mod. Phys.* **85** 1245
[8] Ren X, Yu H Y and Zhang Y 2024 *Acta Phys. Sin.* **73** 047801 (in Chinese)
[9] Feinberg G, Sucher J and Au C K 1989 *Phys. Rep.* **180** 83
[10] Boinovich L and Emelyanenko A 2011 *Adv. Colloid Interface Sci.* **165** 60
[11] Parsegian V A 2005 *Van Der Waals Forces: a Handbook for Biologists, Chemists, Engineers, and Physicists* Cambridge (Published: Cambridge University Press) pp. 47–48

[12] Bordag M, Mohideen U and Mostepanenko V M 2001 *Phys. Rep.* **353** 1
[13] Klimchitskaya G L, Mohideen U and Mostepanenko V M 2009 *Rev. Mod. Phys.* **81** 1827
[14] Woods L M, Dalvit D A R, Tkatchenko A, Rodriguez-Lopez P, Rodriguez A W and Podgornik R 2016 *Rev. Mod. Phys.* **88** 045003
[15] Miao B 2020 *Acta Phys. Sin.* **69** 080505 (in Chinese)
[16] Gong T, Corrado M R, Mahbub A R, Shelden C and Munday J N 2021 *Nanophotonics* **10** 523
[17] Chan H B, Aksyuk V A, Kleiman R N, Bishop D J and Capasso F 2001 *Science* **291** 1941
[18] Shelden C, Spreng B and Munday J N 2024 *Appl. Phys. Rev.* **11** 041325
[19] Hu Y, Wu X, Liu H, Ge W, Zhang J and Huang X 2024 *ACS Photonics* **11** 1998
[20] Munkhbat B, Canales A, Küçüköz B, Baranov D G and Shegai T O 2021 *Nature* **597** 214
[21] Küçüköz B, Kotov O V, Canales A, Polyakov A Y, Agrawal A V, Antosiewicz T J and Shegai T O 2024 *Sci. Adv.* **10** eadn1825
[22] Esteso V, Frustaglia D, Carretero-Palacios S and Míguez H 2024 *Adv. Phys. Res.* **3** 2300065
[23] Ge L, Liu K, Gong K and Podgornik R 2024 *Phys. Rev. Appl.* **21** 044040
[24] Sloan J, Rivera N, Joannopoulos J D and Soljačić M 2021 *Phys. Rev. Lett.* **127** 053603
[25] Li R, Long Y and Zhang X 2025 *Chin. Phys. B* **34** 020307
[26] Li N, Lin Z, Wei M, Liao M, Xu J, Ke S and Yang Y 2023 *Chin. Phys. B* **32** 120301
[27] Li Y, Milton K A, Brevik I, Malyi O I, Thiyam P, Persson C, Parsons D F and Boström M 2022 *Phys. Rev. B* **105** 014203
[28] Esteso V, Carretero-Palacios S, MacDowell L G, Fiedler J, Parsons D F, Spallek F, Míguez H, Persson C, Buhmann S Y, Brevik I and Boström M 2020 *Phys. Chem. Chem. Phys.* **22** 11362
[29] Boström M, Malyi O I, Parashar P, Shajesh K V, Thiyam P, Milton K A, Persson C, Parsons D F and Brevik I 2017 *Phys. Rev. B* **95** 155422
[30] Ge L, Shi X, Li B and Gong K 2023 *Phys. Rev. E* **107** 064402
[31] Baranov M A, Klimchitskaya G L, Mostepanenko V M and Velichko E N 2019 *Phys. Rev. E* **99** 022410
[32] Klimchitskaya G L, Mostepanenko V M and Velichko E N 2020 *Phys. Rev. B* **102** 161405
[33] Klimchitskaya G L, Mostepanenko V M and Velichko E N 2021 *Phys. Rev. B* **103** 245421
[34] Velichko E, Baranov M and Mostepanenko V 2020 *Mod. Phys. Lett. A* **35** 2040020
[35] Mostepanenko V M, Velichko E N and Baranov M A 2020 *J. Electron. Sci. Technol.* **18** 100023
[36] Klimchitskaya G L, Mostepanenko V M and Tsybin O Y 2022 *Symmetry* **14** 2196
[37] Zhao R, Koschny T, Economou E N and Soukoulis C M 2011 *Phys. Rev. B* **83** 075108
[38] Zhou S, Liu K, Dai S and Ge L 2025 *Acta Phys. Sin.* **74** 014202 (in Chinese)
[39] Ge L, Shi X, Xu Z and Gong K 2020 *Phys. Rev. B* **101** 104107
[40] Zhan T, Shi X, Dai Y, Liu X and Zi J 2013 *J. Phys.: Condens. Matter* **25** 215301
[41] Moazzami Gudarzi M and Aboutalebi S H 2021 *Sci. Adv.* **7** 2272
[42] Esteso V, Carretero-Palacios S and Míguez H 2016 *J. Appl. Phys.* **119** 144301
[43] Munday J N, Capasso F and Parsegian V A 2009 *Nature* **457** 170
[44] Ge L, Shi X, Liu L and Gong K 2020 *Phys. Rev. B* **102** 075428
[45] Wang Y, Narayanan S R and Wu W 2017 *ACS Nano* **11** 8421
[46] Zhang C, Li Y, Lin B, Tang J, Sun Q, Xie W, Deng H, Zheng Q and Cheng S 2023 *Chin. Phys. B* **32** 028801
[47] Hu Y, Wu X, Liu H and Huang X 2024 *Nanophotonics* **13** 2983